

## ELECTRICAL DRIVE FOR COMPRESSOR ON TURBOCHARGED ENGINE

Jaroslav Novák<sup>1</sup>, Zdeněk Čerovský<sup>2</sup>

Turbochargers are usually driven by turbine powered by exhausted gases. This conception is relatively simple but the compressor is not able to overcharge the compressed air or fuel-air mixture into the cylinder in the total revolution range and power regimes. Next disadvantage of turbine driven compressor is the low dynamic response of the turbine and compressor at quick fuel supply increase. There are two possible solutions. First - the “electrocharger”, that is the fully electric driven compressor can be used. Second - the hybrid driven charger is possible. Research of supercharging systems is one of activities of Josef Božek Research Centre of Engine and Automotive Technology on Faculties of Mechanical and Electrical Engineering at Czech Technical University in Prague. Part of this activity is research of electrical drive for the hybrid supercharging system especially from control point of view.

Electric synchronous motor with permanent magnets was chosen as electric driving machine. Its robustness, high torque overload features, its small size and mass, high dynamical features and feasible high revolutions are promising for this implementation. Paper deals with torque control of high speed permanent magnet synchronous motor for driving compressor of supercharged combustion engines. Control structure which includes regimes with both full magnetic flux and flux weakening is described. Paper describes the research working place and presents test results achieved on 40 000 rev/min synchronous permanent magnet motor.

**Key words:** high speed drive, synchronous motor, inverter, torque control

### 1 Introduction

Implementation of supercharged combustion engines for automotive, railways or ship traffic offers output power increasing, combustion efficiency improvement, fuel consumption diminishing, better inlet valve and cylinder cooling, and ecological indicating parameters improvements.

Turbochargers are usually driven by turbine powered by exhausted gases. This conception is relatively simple but has several disadvantages. The compressor is not able to overcharge the compressed air or fuel-air mixture into the cylinder in the total revolution range and power regimes. Firstly at low speed the turbine does not produce sufficient power and compressor does not produce sufficient pressure. Vice versa, at high speed the turbine produces surplus power. Next disadvantage of turbine driven compressor is the low dynamic response of the turbine and compressor at quick fuel supply increase. It is

---

<sup>1</sup> doc. Jaroslav Novák, Czech Technical University in Prague, Faculty of Mechanical engineering, Department of Instrumentation and Control Engineering, Technická 4, 166 07 Prague 6, Czech Republic, tel.: +420 224 352 698, E-mail: jaroslav.novak@fs.cvut.cz

<sup>2</sup> prof. Zdeněk Čerovský, Czech Technical University in Prague, Faculty of Electrical Engineering, Department of Electric Drives and Traction, Technická 2, 166 27 Prague6, Czech Republic, tel.: +420 224 352 157, E-mail: cerovsky@fel.cvut.cz

caused because the turbine cannot produce torque and the compressor cannot produce air compression immediately after the fuel supply was increased.

It is obvious that the best solution is to control the compressor in relation to instantaneous revolutions and instantaneous fuel quantity. The dynamic of the drive must agree with the dynamic of fuel supply change and air quantity requirement.

There are two possible solutions. First - the “electrocharger”, that is the fully electric driven compressor can be used. Second - the hybrid driven charger is possible. This solution means that the charger has both turbine drive and electric drive in cooperation. In practise the hybrid driven charger is more advantageous. The electric part of the charger balances the turbine lack of power and improves the system dynamic.

Hybrid drive itself has also two variants. In first variant the electric motor is situated on the common shaft with the turbine and compressor. Electric motor revolutions are the same as turbine and compressor revolutions. In the second variant an additional compressor is added to the turbocharger. This is driven with individual electric motor. In this case the electric motor revolutions are dependent only on the compromise between best compressor revolutions and electric drive possibilities.

Research of supercharging systems is one of activities of Josef Božek Research Centre of Engine and Automotive Technology on Faculties of Mechanical and Electrical Engineering at Czech Technical University in Prague. Part of this activity is research of electrical drive for the hybrid supercharging system especially from control point of view.

Electric synchronous motor with permanent magnets (PMSM) was chosen as electric driving machine. Its robustness, high torque overload features, its small size and mass, high dynamical features and feasible high revolutions are promising for this implementation.

## 2 Research working place

Special testing place of Josef Bozek Research Centre was build at the Faculty of Electrical Engineering. The testing place consists of high speed, frequency controlled induction dynamometer (Fig.1) 2,3kW, 350V, 70 000min<sup>-1</sup>, 0,3Nm.

The tested motor is a high speed two pole PMSM 2,9kW, 400V, 40 000min<sup>-1</sup>, 0,7Nm (Fig.1). IGBT microprocessor controlled inverter (Fig. 2) supplies the PMSM. The control unit TMS320F2812 is additionally completed with the card for PMSM rotor angel position evaluation (Fig.3). The system is equipped with torque calculation from tensometer signals. Chokes of 2,4mH are connected in series with PMSM stator winding to diminish current pulsation. PMSM has integrated two pole resolver used for measuring of rotor position. To evaluate rotor position the electronic unit was developed.

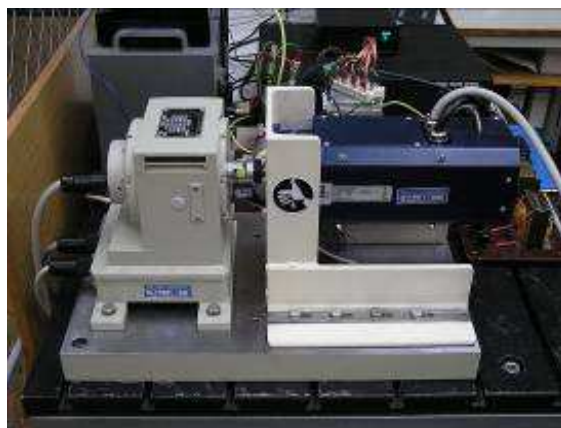


Fig. 1 High speed motor set with induction dynamometer (left) and synchronous motor PMSM (right)

It generates exciting resolver signal 10kHz and gives twelve bit rotor position resolution, that means 4096 positions per one revolution. Information on absolute rotor position is transferred into the controller by serial bus after the controller reset and in still stand. Information on relative rotor position in working mode is transferred in form of IRC sensor signals. Further information on rotor position angel data scanning are explained in [3].

System with controller on base of DSP TMS320F240 was used for torque control till 10 000min<sup>-1</sup> when tests started. System with controller on base of DSP TMS320F2812 was used for torque control in whole revolution range 0 – 40 000 min<sup>-1</sup>.

Invertor switching frequency 5kHz was used in tests with the first control system. Invertor switching frequency 10kHz was used in tests with the second control system in whole revolution range 0 – 40 000 min<sup>-1</sup>. Calculations in the control structure are performed with frequency 15kHz.

At the time when the test place was in construction, dynamometer corresponding with tested PMSM in regards of power, torque and revolutions was not available. Therefore PMSM can be loaded only to quarter of the torque. Nevertheless the control structure can be sufficiently tested.



Fig. 2 Experimental IGBT invertor for high speed drive



Fig. 3 DSP controller of high speed drive with TMS320F2812 and with additional unit for PMSM rotor angel position evaluation

### 3 Theoretical analysis of the torque control

The lowest feedback control level at high speed drive for “electro” charger is the torque control. We started from standard method used for PMSM control.

Standard method for torque control of PMSM goes out from equation Eq.1.

$$M = 1.5 \cdot p_p \cdot (F_d \cdot i_q - F_q \cdot i_d) \quad (1)$$

$F_d$  is magnetic flux linkage component in axis d,  $F_q$  is magnetic flux linkage component in axis q,  $i_d$  is stator current component in axis d,  $i_q$  is stator current component in axis q,  $2p_p$  is number of poles on the machine. Using synchronous machine mathematical model equations we can write Eq. 1 as

$$\begin{aligned} M &= 1.5 \cdot p_p \cdot [(F_f + L_d \cdot i_d) \cdot i_q - L_q \cdot i_q \cdot i_d] = \\ &= 1.5 \cdot p_p \cdot i_q \cdot (F_f + L_d \cdot i_d - L_q \cdot i_d) \end{aligned} \quad (2)$$

$F_f$  is rotor magnetic flux linkage,  $L_d$  is synchronous direct-axis inductance and  $L_q$  is synchronous quadrature-axis inductance. If machine works in full magnetic flux regime the  $i_d$  (stator current component in axis d) equals zero and for the torque holds

$$M = 1.5 \cdot p_p \cdot F_f \cdot i_q \quad (3)$$

Eq. 3 holds for field weakening regime too when  $L_d=L_q$ . This equality is usually fulfilled on PMSM. In field weakening regime  $i_d$  (stator current component in axis d) acts against permanent magnet flux and enables to operate the machine in high revolutions with constant stator voltage.

Eq. 3 express analogy with DC machine. Current and torque control can be performed either in transformed coordinates or by controlling instantaneous stator current with respect to instantaneous rotor position. In regime of full magnetic flux the current of given phase is controlled in such a way that the current amplitude occurs in time when the rotor is perpendicular with this phase. Other current values in remaining phases are  $120^\circ$  shifted. The stator current space vector is  $90^\circ$  ahead of the rotor.

Torque control with instantaneous current control in stator phases was implemented. It was tested up to  $10\,000\text{ min}^{-1}$  with controller based on TMS320F240. After adding controller parameter adaptation and using operational values prediction (referential voltage values on PWM modulator input) good results were achieved as shown in[2].

Space stator current vector of  $i_d$  (stator current component in axis d) acts against permanent magnets magnetomotive force (MMF) in field weakening regime. With other words the space vector  $i_d$  is  $90^\circ$  ahead according to the stator induced voltage  $U_i$ . That means the voltage drop  $j\omega L_d i_d$  has orientation against the induced voltage vector  $U_i$ . Generally in weakening regime and when  $L_d=L_q=L_1$ , the phasor diagram on Fig. 4 shows this situation. In full flux regime equals  $i_d$  to zero and the space stator current vector lies in quadrature axis q. In Fig. 4 is  $R_1$  stator winding resistance, and  $U_i$  is the induced voltage.

### 4 Structure of feedback torque control and its implementation

The torque control structure of PMSM implemented for tests of the high speed drive  $40\,000\text{min}^{-1}$  uses the controller based on TMS320F2812.

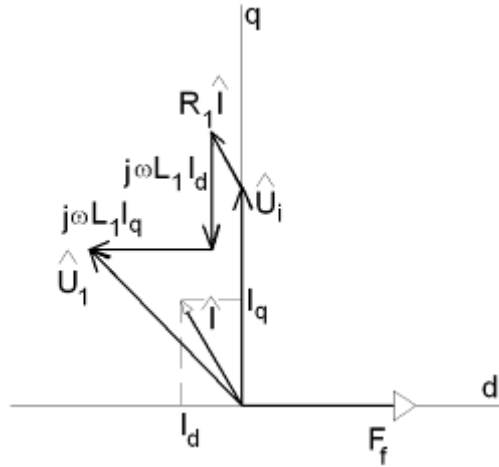


Fig. 4 Phasor diagram of synchronous engine at torque control.

It works in orthogonal coordinate system d-q and cooperates with appropriate transformation blocks. Block scheme is shown in Fig. 5. Regime with field weakening is not assumed for “electric” charger. Nevertheless it is involved into the control structure for  $40\,000\text{min}^{-1}$  for the substance of the control structure is the linear vector axis q) and flux current component  $i_d$  (stator current component in axis d) are controlled separately. Desired torque current component  $i_q$  is calculated from required torque and desired flux current component  $i_d$  in full magnetic flux regime equals to zero. PMSM torque control in orthogonal coordinate system. Torque current component  $i_q$  (stator current component in reasons of continuous control till  $40\,000\text{min}^{-1}$  or more respectively for reason of inverter supply voltage fluctuation.

Actual current components  $i_U$  and  $i_V$  are measured and  $i_d$  and  $i_q$  are calculated from measured stator currents and rotor position angle  $\varphi$ . Standard equations are used:

$$\begin{aligned}
 i_\alpha &= i_U \\
 i_\beta &= \frac{i_V - i_W}{\sqrt{3}} = \frac{i_U + 2i_V}{\sqrt{3}} \\
 i_d &= i_\alpha \cos \varphi + i_\beta \sin \varphi \\
 i_q &= -i_\alpha \sin \varphi + i_\beta \cos \varphi
 \end{aligned} \tag{4}$$

Outputs of current controllers of current components  $i_q$ ,  $i_d$  are stator voltage components  $u_q$ ,  $u_d$ . These components are transformed in transformation blocks into referential phase voltages using instantaneous angle  $\varphi$  values by standard equations:

$$\begin{aligned}
 u_\alpha &= u_d \cos \varphi - u_q \sin \varphi \\
 u_\beta &= u_d \sin \varphi + u_q \cos \varphi \\
 u_U &= u_\alpha \\
 u_V &= \frac{\sqrt{3} \cdot u_\beta - u_\alpha}{2} \\
 u_W &= -u_U - u_V
 \end{aligned} \tag{5}$$

It is possible to activate the block “Modulation index correction” before introducing referential values of phase voltages into PWM modulator. This block modifies modulator input values to reach maximum possible first harmonics of stator phase voltage no matter what the DC voltage is.

The pulse width modulator PWM generates pulses to control IGBT with switching frequency 10kHz. Algorithms for field weakening mode are a superset to the basic control structure. In this case the control structure generates nonzero demagnetizing required current component  $i_d^*$ . This current component ensures that the maximum amplitude of referential voltage signal into the PWM modulator remains constant.

It was maintained approximately at 85% of the maximum value during tests.

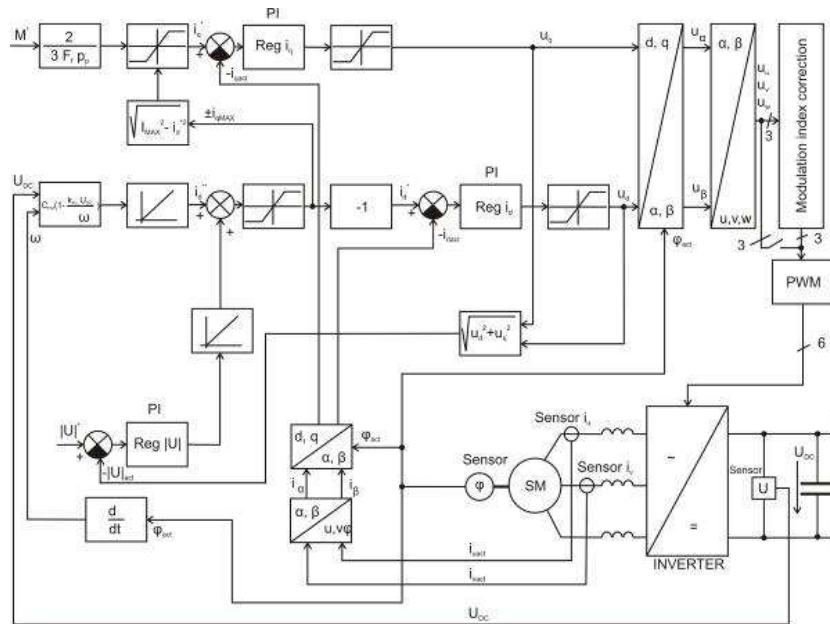


Fig.5 Torque structure control of high speed drive

Required value  $i_d^*$  is a sum of the output of a PI voltage controller and of  $i_d^{**}$  - calculating block designed for compensating the part of motor voltage that exceeds the maximal acceptable stator voltage. (With other words  $i_d^{**}$  is calculated to compensate the exceeding part of motor induced voltage and of the maximal outgoing inverter voltage for actual DC voltage and actual revolutions).

This calculating block makes the control faster in transient events.

Basic behaviour of the described block is established on the following idea: the increment of induced voltage which should be eliminated by current component  $i_d^{**}$  after shifting in weakening field regime is given by equation:

$$\Delta U_i = L_d \cdot i_d \cdot \omega = k_\Phi \cdot F_f \cdot (\omega - \omega_{pr}) \quad (6)$$

In Eq. 6  $L_d$  is stator inductance in axis d,  $\omega$  is mechanical angular velocity in electric degrees,  $k_\Phi$  is motor constant determining relation between rotor magnetic flux and stator induced voltage and revolutions, and  $\omega_{pr}$  is angular velocity at which the passing from full magnetic flux into weakening field regime begins at given input inverter voltage in no-load. Assuming changing DC input voltage for the inverter the value of  $\omega_{pr}$  for no-load regime is given by Eq. 7

$$\omega_{pr} = k_{pu} \cdot U_{DC} \quad (7)$$

$k_{pu}$  is constant of proportionality and  $U_{DC}$  is input voltage into the inverter. By arrangement of Eq. 6 and 7 we get for current component  $i_d^{**}$ , which eliminates stator voltage increment in weakening field regime:

$$i_d^{**} = C_{FM} \cdot \left(1 - \frac{k_{pu} \cdot U_{DC}}{\omega}\right) \quad (8)$$

For  $C_{FM}$  it holds:

$$C_{FM} = \frac{k_{\Phi} \cdot F_f}{L_d} \quad (9)$$

PI voltage controller gives on its output required current component  $i_d$ , which creates sufficient voltage reserve on the inverter output to cover the voltage drop on stator impedances at torque changing. The real voltage amplitude value for control error is calculated by Pythagoras formula.

The used conception for current component  $i_d$  calculation in field weakening mode respects the implementation necessity which demands to accomplish all calculations in real time. In case of high speed drive, real time for total control structure calculation is short. Therefore the calculation  $i_d^{**}$  value from Eq. 8 respects only the induced voltage increment and not the voltage drop at load changes. To respect the total voltage drop on stator impedance in this block would mean to increase the computing power requirements over the limits of the DSP.

The advantage of this control method is the smooth passing from full magnetic flux into weakening field regime. Algorithm for weakening field regime is active in full magnetic flux regime too but the required value  $i_d^*$  is zero. The total motor current is geometrical sum of currents  $i_d$  and  $i_q$ . The total current cannot get over the current limitation. Under this conditions the special block used in the control structure begins to diminish the torque component  $i_q$  not to get over the current limitation. The control structure works with the frequency 15kHz. The main part of the control is performed in interrupt and is implemented in assembler language. The logic control of the drive (regime switching or parameters settings for example) and developing support are implemented in C language against background. The time reserve for calculation at PWM modulation with 10kHz was approximately 10-20%. To enlarge this reserve the reduction of program code and development environment support would be necessary. But this would not bring much improvement as it can raise the PWM frequency but this will heighten the switching losses and it will diminish the inverter efficiency.

## 5 Test experiments

Experiments were performed on high speed motor set and induction dynamometer depicted in Fig. 1. Starting up of the motor without loading torque and with different torque loads were measured and evaluated. Further measurements at constant revolutions under different loads were performed. Constant revolutions were controlled by speed loopback of the dynamometer. Load experiments were limited by dynamometer low torque.

In Fig. 6 are depicted curves measured at no load starting up till 40 000  $\text{min}^{-1}$  at torque 0,44Nm without modulation index correction ( $i_q=5,7\text{A}$ ) Depicted are actual current components  $i_q$ ,  $i_d$ , revolutions in frequency scale (Hz/100), amplitude of reference voltage introduced into PWM modulator in per unit values (maximum=10). In Fig. 7 are depicted the same values at the same starting up but with modulation index correction.

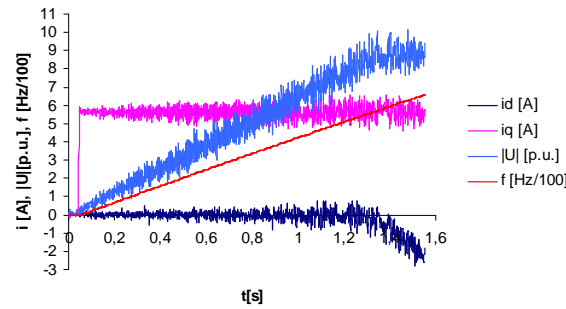


Fig. 6. Current components  $i_d$ ,  $i_q$ , amplitudes of reference voltage and frequency (revolutions) at no load starting up till  $40\,000\text{ min}^{-1}$  at torque  $0,44\text{Nm}$  without modulation index correction.

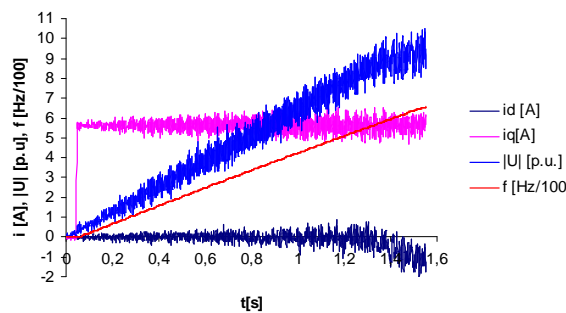


Fig. 7. Current components  $i_d$ ,  $i_q$ , amplitudes of reference voltage and frequency (revolutions) at no load starting up till  $40\,000\text{ min}^{-1}$  at torque  $0,44\text{Nm}$  with modulation index correction.

In Fig. 8 and 9 are depicted other examples of  $i_d$ ,  $i_q$ , current components, revolutions in frequency scale (Hz/100), amplitude of reference voltage introduced into PWM modulator in per unit values (maximum=10) without modulation index correction during no load starting up. During these starting up was the required torque changed what can be seen in different revolution curves.

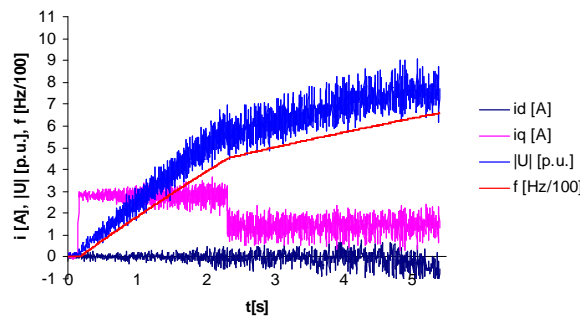


Fig. 8. Curves of current components  $i_d$ ,  $i_q$ , amplitude reference voltage and revolutions (frequency) during no load starting up till  $40\,000\text{ min}^{-1}$  at load torque changing suddenly from  $0,22\text{Nm}$  to  $0,11\text{Nm}$



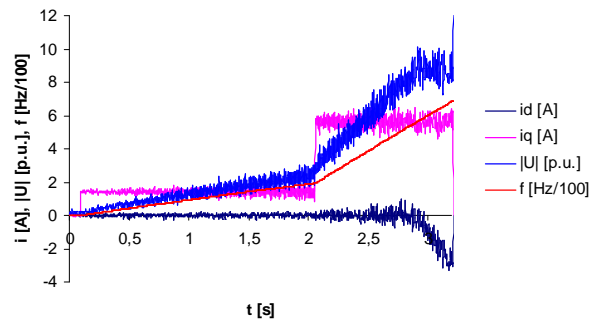


Fig. 9. Curves of current components  $i_d$ ,  $i_q$ , amplitude reference voltage and revolutions (frequency) during no load starting up till  $40\,000\text{ min}^{-1}$  at load torque changing suddenly from  $0,11\text{Nm}$  to  $0,44\text{Nm}$

It can be seen from Fig. 6, 7, 8, 9 that with revolutions (that is with frequency) going up the ripple of current components  $i_d$ ,  $i_q$  and reference voltage amplitude ripple are going up too. That is caused by the fact that simultaneously the PWM number of periods is decreasing and the action signals in one period of outgoing first harmonic voltage from the converter is decreasing also.

In Fig. 10 and 11 are details of drive quantities in short time sections depicted. In Fig. 10 is detail of starting up in the very beginning at accelerating torque of  $0,44\text{Nm}$ . Depicted are  $i_d$ ,  $i_q$ , amplitude of reference voltage and revolutions. In Fig. 11 are curves of drive quantities after quickly changed torque from 0 to  $0,11\text{Nm}$  at  $40\,000\text{ min}^{-1}$  depicted.

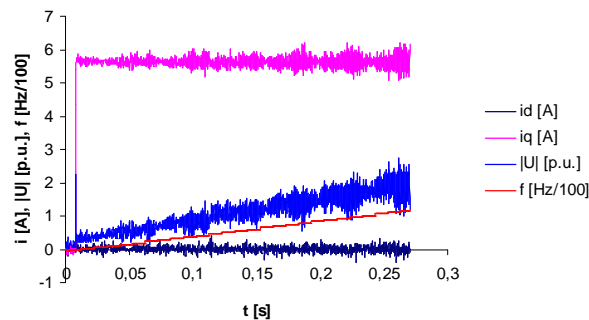


Fig. 10. Detail after quickly changed torque from 0 to  $0,44\text{Nm}$  at constant revolutions  $40\,000\text{min}^{-1}$ .

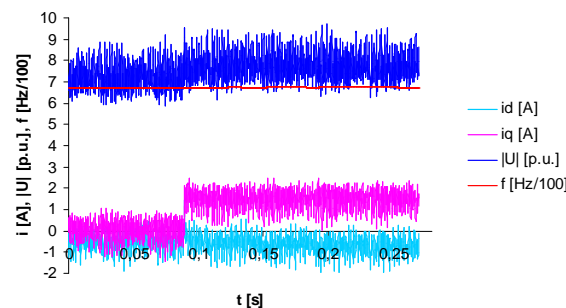


Fig. 11. Detail after quickly changed torque from 0 to  $0,11\text{Nm}$  at constant revolutions  $40\,000\text{min}^{-1}$

## 6 Conclusion

High Speed Synchronous Motor Control for electrically driven compressors on overcharged gasoline or diesel engines was tested in laboratory. Experiments showed good features of the control structure. Only during very quick starting up of the drive a lag in the control loop of reference voltage amplitude was observed. It was not important for so quick starting up regimes.

The research will continue with experiments together with real mechanical load by compressor and with respect to combustion engine needs.

Overcharging compressors used for high power combustion engines have revolutions round 40 000 min<sup>-1</sup> or more. Combustion engines for automobiles need higher revolutions round 100 000 min<sup>-1</sup> or more. In further research also this “electrochargers” must be taken into account.

## Reference literature

1. Novotny D.W., Lipo T.A.: Vector Control and Dynamics of AC Drives, Oxford Science Publications Nr 41, 1996
2. Čeřovský Z., Novák J., Novák M., Čambál M.: Digital Controlled High Speed Synchronous Motor, EPE PEMC Conference, Poznaň, Poland 2008.
3. Čambál, M. - Novák, M. - Novák, J.: Study of Synchronous Motor Rotor Position Measuring Methods. In 13th International Conference on Electrical Drivers and Power Electronics. Zagreb, Croatia: KoREMA, 2005, p. 62-66. ISBN 953-6037-42-4.
4. Lettl, J., Fligl, S.: Matrix Converter in Hybrid Drives. Proceedings of 8th International Conference “Problems of Present-day Electrotechnics, PPE 2004”, Vol. 3, pp. 77-80, Kyiv, 2004, ISSN 0204-3599.
5. Lettl, J., Fligl, S., Kuzmanovic, D.: Comparison of Different Types of AC/AC Converters. Electronics Device and Systems IMAPS CS International Conference EDS 2006 Proceedings, pp. 427-432, Brno, 2006, ISBN 80-214-3246-2